Available online at www.sciencedirect.com
ScienceDirect
Applied Catalysis A: General 318 (2007) 63–69
APPLIED CATALYSIS A: GENERAL
www.elsevier.com/locate/apcata

Carbon nanotubes synthesis by the ethylene chemical catalytic vapour deposition (CCVD) process on Fe, Co, and Fe–Co/Al_2O_3 sol–gel catalysts

Kim Yên Tran [a], Benoît Heinrichs [a,*], Jean-François Colomer [b], Jean-Paul Pirard [a], Stéphanie Lambert [a]

[a] *Laboratoire de Génie Chimique, B6a, Université de Liège, Sart-Tilman, B-4000 Liège, Belgium*
[b] *Laboratoire de Résonance Magnétique Nucléaire of the Facultés Universitaires Notre-Dame de la Paix, B-5000 Namur, Belgium*

Received 30 June 2006; received in revised form 29 September 2006; accepted 20 October 2006
Available online 30 November 2006

Abstract

The production of carbon nanotubes by the chemical catalytic vapour deposition, CCVD, process was examined over iron, cobalt, and a mixture of iron and cobalt supported on alumina catalysts synthesized by a one step sol–gel process. The catalysts were synthesized from several metal precursors, iron nitrate, cobalt and iron acetylacetonate, and cobalt acetate. Ethylene was used as the carbon source.

The Co/Al_2O_3 catalysts showed better activity and selectivity in carbon nanotubes synthesis than Fe/Al_2O_3 and Fe–Co/Al_2O_3 catalysts. The carbon deposit was found by TEM analysis to be rich in carbon nanotubes in the case of Co/Al_2O_3 but to be very poor in the case of the Fe–Co/Al_2O_3 catalysts. The catalysts were characterized by TEM, XRD, and nitrogen adsorption. It was shown that iron and cobalt are in oxide form. Metal–support interactions and metal oxide particle size are influenced by the nature of the precursor and this nature is an important factor for the activity and selectivity of the catalysts. Moreover, a correlation has been found between the metal oxide particle sizes, the diameter of the carbon nanotubes, and the catalytic activity.

Keywords: Carbon nanotubes; Sol–gel; Metal precursors; Ethylene; Chemical catalytic vapour deposition

1. Introduction

Hollow carbon fibres have been observed for several decades [1], but it was the groundbreaking report by Ijima [2] that made carbon nanotubes one of the most actively investigated category of materials. Their unique structural, electronic, mechanical, electromechanical, and chemical properties lead to extensive research on their potential applications [3]. In spite of this interest, the lack of sufficient material limited the research on their properties and applications. The scaling-up of carbon nanotubes production remains a challenge.

Several methods exist for the synthesis of carbon nanotubes. Typically, they are prepared by arc-discharge, laser ablation, or chemical catalytic vapour deposition process, CCVD [4]. The chemical catalytic vapour deposition process has been used for the preparation of single and multi-walled carbon nanotubes by catalytic decomposition of various hydrocarbons. The principal hydrocarbons used are acetylene, ethylene, and methane. This method is more easily scaled up [5,6], is less expensive because it proceeds at moderate temperatures of less than 1000 °C, and is reported to have a high yield [4], to produce low defects carbon nanotubes [7], and to yield longer carbon nanotubes than does arc-discharge and laser ablation [8].

Because the chemical catalytic vapour deposition process seems to be the most fitted method for producing large scale carbon nanotubes, research on new effective catalysts is essential. Catalysts used in chemical catalytic vapour deposition process for the synthesis of carbon nanotubes are usually iron, cobalt, or nickel-supported catalysts prepared by impregnation [9], co-precipitation [10], or sol–gel processes [11].

The choice of the supporting material has been found to be critical. Indeed, the nature of the support, Al_2O_3, SiO_2, or MgO, its surface area, porosity, and the dispersion of the transition metal particles can influence the carbon nanotube productivity.

* Corresponding author. Tel.: +32 4366 3505; fax: +32 4366 3545.
E-mail address: b.heinrichs@ulg.ac.be (B. Heinrichs).

0926-860X/$ – see front matter © 2006 Elsevier B.V. All rights reserved.
doi:10.1016/j.apcata.2006.10.042

Nomenclature

d_{CNTs}	the average carbon nanotubes size calculated from the observation of 30 carbon nanotubes
d_{min}	the minimum diameter of metal particle, the minimum carbon nanotubes diameter
d_{max}	the maximum diameter of metal particle, the maximum carbon nanotubes diameter
d_{TEM}	the average metal particle size calculated from the observation of 150 particles by TEM
d_{XRD}	the average metal particle size calculated from XRD patterns
S_{BET}	the specific surface area of the catalyst measured by the BET method

The sol–gel method seems to be a very appropriate way to synthesize catalyst supports because it yields high surface area supports with high porosity, properties that facilitate the high dispersion of metal particles during the later impregnation step [12]. Furthermore, the sol–gel method permits metal-supported catalysts synthesis in one step that means that the dispersion of metal precursors takes place during the support synthesis by sol–gel. Other than the convenience of saving a step, one step sol–gel method may also introduce unique metal–oxide interactions [13] or oxide–oxide interactions [14] that are inaccessible with other preparative methods.

Purification after the synthesis process is a very important part of the carbon nanotubes production process. It involves the separation and the removal of catalyst particles, support material, and amorphous particles from carbon nanotubes. The catalyst support removal is the most problematic. The use of aluminium oxide catalyst support simplifies somewhat the purification process because it is soluble in concentrated alkali solutions.

Therefore, novel Fe/Al_2O_3, Co/Al_2O_3, and $Fe–Co/Al_2O_3$ catalysts have been prepared to produce carbon nanotubes by the chemical catalytic vapour deposition process with ethylene as the carbon source. These catalysts were synthesized by a one step sol–gel method adapted to iron and cobalt from the Kim et al. method [15] for the synthesis of Pd/Al_2O_3 three-way catalysts. Iron acetylacetonate, $Fe(CH_3COCH{=}C(O)CH_3)_3$ or $Fe(acac)_3$, and iron nitrate, $Fe(NO_3)_3$, have been used as the iron precursors and cobalt acetylacetonate, $Co(CH_3COCH{=}C(O)CH_3)_2$ or $Co(acac)_2$, and cobalt acetate, $Co(C_2H_3O_2)_2$ or $Co(OAc)_2$, have been used as the cobalt precursors.

2. Experimental

2.1. Catalyst synthesis

Two Fe/Al_2O_3, two Co/Al_2O_3 and two $Fe–Co/Al_2O_3$ xerogel catalysts have been prepared. The initial solution contains the support precursor, aluminium isopropoxide, $Al(C_3H_7O)_3$, and the metal precursor. In order to investigate the influence of the nature of the metal precursor, different precursors have been used, namely $Fe(acac)_3$ and $Fe(NO_3)_3$ for the iron catalysts and $Co(acac)_2$ and $Co(OAc)_2$ for the cobalt catalysts. Bimetallic catalysts were synthesized from mixtures of either $Fe(NO_3)_3$ and $Co(OAc)_2$ or from mixtures of $Fe(acac)_3$ and $Co(acac)_2$.

Table 1
Designation, precursors, and metal loading of the xerogel catalysts synthesized from $Al(C_3H_7O)_3$

Designation	Metal precursors	Metal loading
F1	$Fe(NO_3)_3$	4 wt% Fe
F2	$Fe(acac)_3$	4 wt% Fe
C1	$Co(OAc)_2$	4.21 wt% Co
C2	$Co(acac)_2$	4.21 wt% Co
FC1	$Fe(NO_3)_3$ and $Co(OAc)_2$	1.95 wt% Fe and 2.06 wt% Co
FC2	$Fe(acac)_3$ and $Co(acac)_2$	1.95 wt% Fe and 2.06 wt% Co

The designation, precursors, and metal loading of the six samples studied herein are given in Table 1. The metal loading of the iron catalysts is 4 wt%, which corresponds to 0.7×10^{-3} mol of iron per gram of catalyst. Because of the need to compare the different catalysts, the total amount of metal in each catalyst has been kept constant at 0.7×10^{-3} mol of metal per gram of catalyst. It should be noted that the iron to cobalt molar ratio in FC1 and FC2 is 1:1.

The $Al(C_3H_7O)_3$ support precursor was dissolved in water in a proportion $n_{water} : n_{Al(C_3H_7O)_3}$ of 100:1 and the solution was stirred for 1 h. Then, a 1.5 M aqueous ammonia solution was added under stirring until the pH of the resulting solution reaches a value of 10. The metal precursor, previously dissolved in acetone, was then added to the first solution. The volume of acetone is calculated so that $V_{acetone} = 1.1 \times (V_{water} + V_{ammonia})$, where V_{water} is the volume of water in the $Al(C_3H_7O)_3$ solution and $V_{ammonia}$ is the volume of 1.5 M ammonia solution. This final solution was stirred for 4 h at 50 °C and then aged for 15 h in a closed flask at ambient temperature. The flasks were then opened and held at ambient temperature for 3 days after which they were dried at 150 °C for 24 h. The catalysts were then calcined in an oven with natural air circulation at 500 °C for 1 h. Each catalyst was crushed and kept in a closed flask.

2.2. Carbon nanotubes synthesis

Catalytic tests were carried out in a fixed bed horizontal quartz tube reactor with an external diameter of 50 mm, an internal diameter of 46 mm and a length of about 880 mm. The 0.5 g of crushed catalyst was disposed in a quartz boat and moved into the reactor. The 0.5 g catalyst bed was 10 mm in width and 200 mm in length. Under these conditions, the reactor works in chemical regime [16]. After purging the reactor with 2.23 mmol s^{-1} of helium for 10 min, the reaction was carried out at 700 °C for 15 min in a mixture of 0.223 mmol s^{-1} of C_2H_4 and 0.521 mmol s^{-1} of He. The carbon deposit obtained was calculated as follows:

$$\text{carbon deposit}\,(\%) = \frac{m_{out} - (m_{in} - \Delta m)}{m_{in} - \Delta m} \times 100,$$

Table 2
Catalysts metal particle diameter and specific surface area

Sample	Pretreatment	Transmission electron microscopy				XRD	
		d_{min} (nm)	d_{max} (nm)	d_{TEM} (nm)	σ (nm)	d_{XRD} (nm)	S_{BET} (m^2/g)
F1-d	Dried + blank test	3	9	4	1.7	6	195
F1-dc	Dried + calcined + blank test	4	15	7	2.9	5	320
F2-d	Dried + blank test	3	10	3	1.6	–[a]	105
F2-dc	Dried + calcined + blank test	2	13	5	1.0	–[a]	295
C1-d	Dried + blank test	2	10	5	2.3	2	240
C1-dc	Dried + calcined + blank test	3	10	5	2.8	3	220
C2-d	Dried + blank test	3	13	8	1.5	9	230
C2-dc	Dried + calcined + blank test	3	17	12	2.9	10	270
FC1-d	Dried + blank test	1	10	5	3.7	–[a]	205
FC1-dc	Dried + calcined + blank test	2	13	8	3.8	–[a]	210
FC2-d	Dried + blank test	1	6	3	4.1	–[a]	165
FC2-dc	Dried + calcined + blank test	2	6	4	1.4	–[a]	235

d_{min}, the minimum diameter; d_{max}, the maximum diameter; d_{TEM}, the average metal particle size calculated from the observation of 150 particles by TEM; d_{XRD}, the average metal particle size calculated from XRD patterns; S_{BET}, the specific surface area measured by the BET method; σ, the standard deviation.
[a] No peak is detected.

where m_{out} is the sum of the deposited carbon mass and catalyst mass after reaction, m_{in} the catalyst mass before reaction, and Δm is the catalyst mass loss at the reaction temperature as a result of residual solvent evaporation. The mass loss was calculated from a blank test in which the catalyst is subjected to the same conditions as during the catalytic test but under a flow of only helium.

Each catalyst was examined for carbon nanotubes synthesis both after drying and after drying and calcination. Each catalyst was characterized after drying and blank test at 700 °C or after drying, calcination and blank test at 700 °C. Dried catalysts are denoted by the letter 'd' and dried and calcined catalysts are denoted by the letters 'dc'.

2.3. Materials characterization

Metal particle sizes and carbon nanotubes diameters have been determined by transmission electron microscopy (TEM) with a Philips CM100 electron microscope. 10 mg of fresh catalyst or catalyst plus the carbon deposit mixture were dispersed in 5 ml ethanol and sonicated for 4 h. A few drops of the resulting suspension were placed on a formwar covered copper grid [17].

Carbon nanotubes diameter has also been observed by HRTEM. A few mg of carbon nanotube sample were dispersed in ethanol, and one droplet was put onto a holey carbon grid, left to dry, and examined in a JEOL 200 CX microscope working at 200 kV.

X-ray diffraction (XRD) was also used to determine the metal particle size and to determine the composition of the catalysts. The patterns were obtained with nickel filtered Cu Kα radiation on hand-pressed samples mounted on a Siemens D5000 goniometer.

The texture of the catalysts was determined, after out gassing for 18 h at ambient temperature, from nitrogen adsorption–desorption isotherms measured at 77 K on a Fisons Sorptomatic 1990.

3. Results

3.1. Catalysts characterization

TEM characterization has been carried out on the catalysts after the blank test at 700 °C. The mean size of active metal particles, d_{TEM}, corresponds to the average for 150 particles of each catalyst; the resulting values are given in Table 2. The metal particle size distribution is continuous between the minimal diameter, d_{min}, and the maximal diameter, d_{max}.

The crystalline phases present in the catalysts have been determined by XRD after blank test at 700 °C. The diffractograms are shown in Figs. 1–3. Intense peaks corresponding to the Al_2O_3 support are observed for all the catalysts. The alumina is present either in the η-Al_2O_3 form or as a mixture of η-Al_2O_3 and γ-Al_2O_3. Metal oxide peaks were observed in catalyst F1 at θ ~33°, ~36°, ~50°, and ~54°, indicating the presence of α-Fe_2O_3 particles. In the case of the F2 catalysts, no peaks corresponding to the iron containing phases are observed, indicating that the iron is highly dispersed on the surface of this catalyst and that the iron oxide containing particles are too small to be detected or that the particles are of amorphous nature. The X-ray diffraction patterns of the cobalt catalyst, C2, indicate the presence of Co_2AlO_4 and/or Co_3O_4 reflections at θ ~31°, ~37°, and ~61°. It is worth noting that the green colour of the C2-d and C2-dc catalysts indicate the presence of Co_2AlO_4. In the case of C1 catalysts, no peaks corresponding to cobalt containing phases are observed. In the bimetallic FC1 and FC2 catalysts, iron and cobalt oxide containing phases are not detected, probably because of their small particle sizes. In all cases, calcination induces an increase in the reflection peak intensities.

The average metal particle size was determined from the X-ray diffraction line broadening by using the Scherrer formula [18] and the results are summarized in Table 2. The F1 and C2 metal particle sizes measured by XRD and by TEM are in good

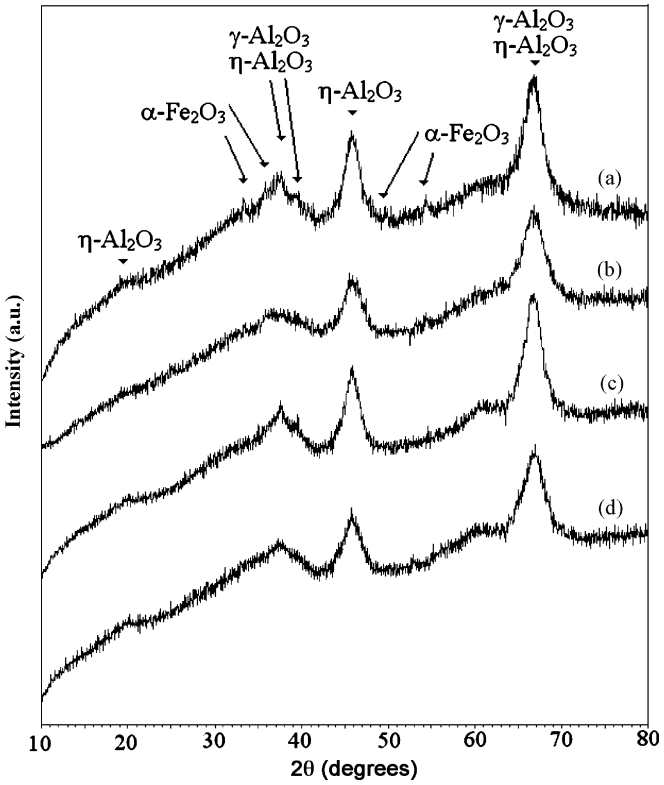

Fig. 1. Diffractograms obtained by XRD of the Fe/Al_2O_3 catalysts after blank tests: (a) F1-dc, (b) F1-d, (c) F2-dc, and (d) F2-d.

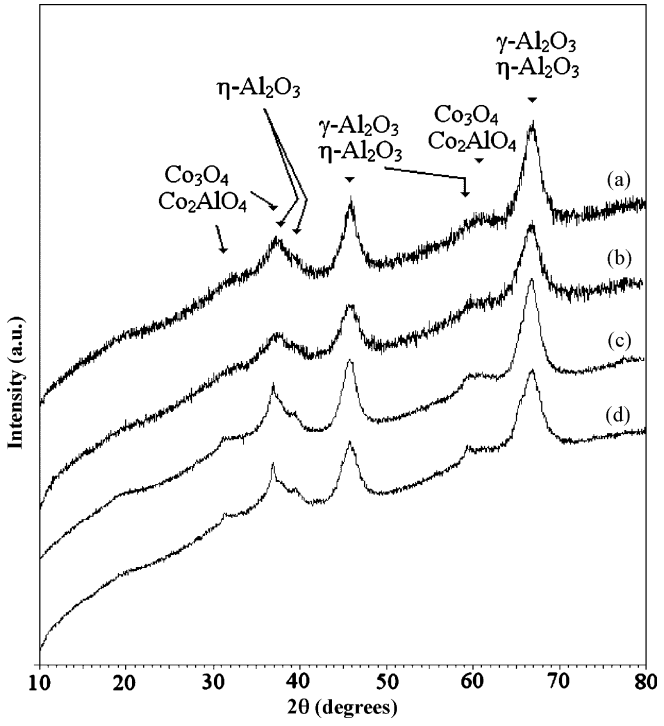

Fig. 2. Diffractograms obtained by XRD of the Co/Al_2O_3 catalysts after blank tests: (a) C1-dc, (b) C1-d, (c) C2-dc, and (d) C2-d.

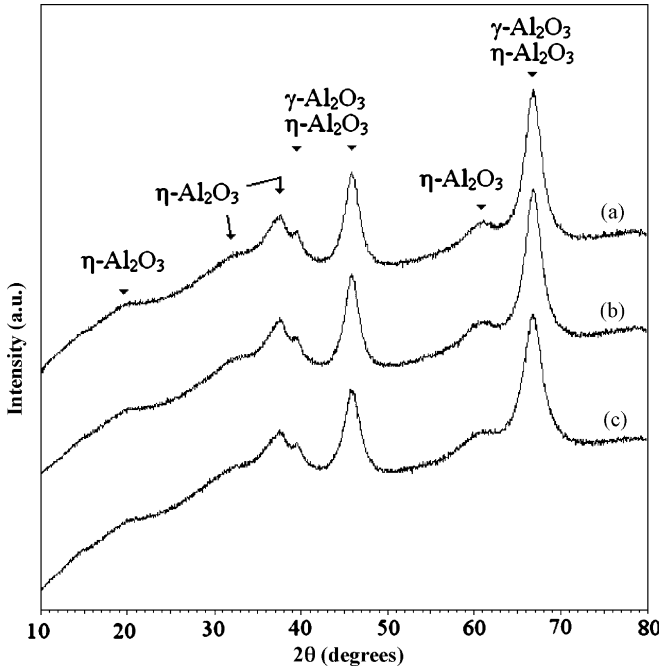

Fig. 3. Diffractograms obtained by XRD of the $Fe–Co/Al_2O_3$ catalysts after blank tests: (a) FC1-dc, (b) FC2-dc, and (c) FC2-d.

agreement. In the case of C1, the metal particle sizes measured by XRD are smaller than those measured by TEM.

Fig. 4 shows the adsorption–desorption isotherm obtained on catalyst C2-dc after the blank test. Similar isotherms are obtained for all samples, dried and dried and calcined. These isotherms are of type IV with a type E hysteresis at low pressure and a type A hysteresis at high pressure near saturation. The mesopore volume distribution is very large ranging from 2 to 50 nm. The presence in the samples of both a micro- and a meso-porosity is indicated by the shape of the *t*-plots, i.e., a downward followed by an upward deviation from the straight line (not shown). The specific surface areas are high and increase after calcination. This increase of the specific surface area may correspond to the removal of the residual solvents present mainly in the micropores [19].

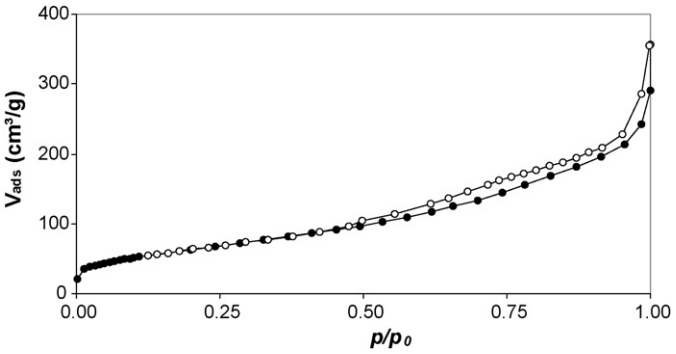

Fig. 4. Nitrogen adsorption–desorption isotherm of the C2-dc catalyst obtained after blank test at 700 °C; (●) corresponds to the adsorption isotherm; (○) corresponds to the desorption isotherm.

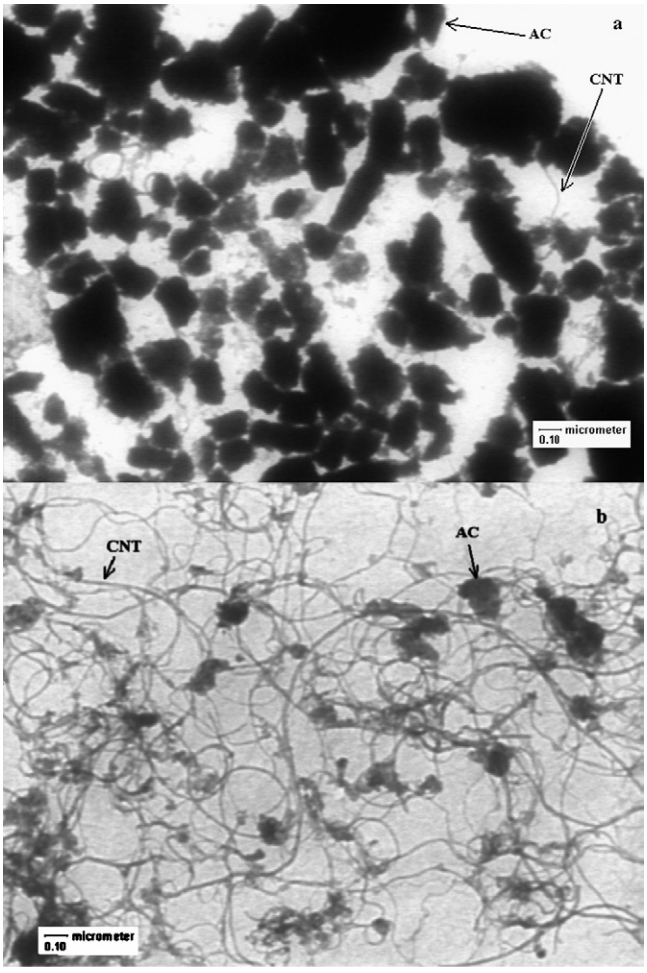

Fig. 5. TEM micrographs of the carbon deposit of (a) FC2-dc and (b) C2-dc (57,750×); CNT indicates a carbon nanotube and AC indicates amorphous carbon.

3.2. Carbon nanotubes characterization

TEM analysis shows that all catalysts produce not only carbon nanotubes but also amorphous carbon. This is illustrated in Fig. 5 with TEM micrographs of the C2-dc and FC2-dc catalysts. Clearly, it appears that C2-dc produces much less amorphous carbon than does FC2-dc. The TEM micrographs of the catalysts producing very weak quantities of carbon nanotubes, i.e., F2-d and F2-dc and FC2-d, are similar to Fig. 5a. The TEM micrographs of the catalysts producing notable quantities of carbon nanotubes, i.e., dried and dried and calcined F1, C1, C2, FC1, are similar to Fig. 5b.

HRTEM analysis shows that the produced carbon nanotubes are multi-walled as it can be seen in Fig. 6 for F1-dc catalyst.

The carbon deposit includes both carbon nanotubes and amorphous carbon. The results presented in Table 3 indicate both that a higher deposit is generally obtained when catalysts are calcined and that cobalt leads to higher deposits than iron. Bimetallic Fe–Co catalysts are generally less active than the monometallic catalysts.

A qualitative carbon nanotube to amorphous carbon ratio has been estimated from the TEM micrographs, see Table 3. This estimate provides an appreciation of the selectivity of the catalyst towards carbon nanotube formation. A correlation seems to exist between the carbon deposit and the carbon nanotube to amorphous carbon ratio. Indeed catalysts with a high carbon deposit, i.e., C2-dc, had a higher carbon nanotubes selectivity than catalysts with a low carbon deposit, i.e., FC2-dc. The carbon nanotubes synthesized are straight or curved with no embranchments. In the case of C1 and C2 cobalt catalysts, some helicoidal nanotubes can be observed as can be seen in Fig. 7. The diameter of the carbon nanotubes obtained with the different catalysts is reported in Table 3.

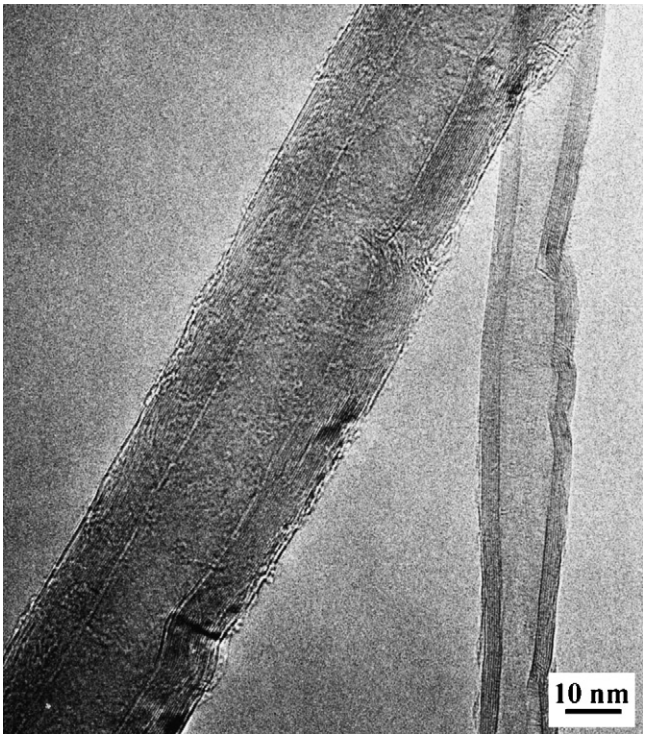

Fig. 6. HRTEM micrograph of the carbon deposit of F1-dc.

4. Discussion

Significant differences in the size of metal particles exist between the various catalysts, differences that could be a consequence of the various metal precursors used, i.e., $Fe(acac)_3$ and $Fe(NO_3)_3$ for the iron catalysts and $Co(acac)_2$ and $Co(OAc)_2$ for the cobalt catalysts. In Table 2, it can be observed that F1 synthesized from $Fe(NO_3)_3$ has larger active metal particles, particles which have average d_{TEM} diameters of 4 and 7 nm for F1-d and F1-dc, respectively, than does F2 synthesized from $Fe(acac)_3$, which have average diameters of 3 and 5 nm for F2-d and F2-dc, respectively. Similarly, C2 synthesized from $Co(acac)_2$ yields larger active metal particles, particles that have average diameters of 8 and 12 nm for C2-d and C2-dc, respectively, than does C1 synthesized from $Co(OAc)_2$, which has average diameters of 5 and 5 nm for C1-d and C1-dc, respectively. The nature of the metal precursor influences the metal particle growth during the sintering process. Indeed, the presence of some anions on the surface

Table 3
Carbon nanotubes diameters obtained by TEM, carbon deposit and selectivity

Sample	Pretreatment	d_{min} (nm)	d_{max} (nm)	d_{CNTs} (nm)	Carbon deposit (%)	Carbon nanotubes/amorphous carbon ratio (m^3/m^3)
F1	Dried	5	18	7	23	High
F1	Dried and calcined	4	24	10	43	High
F2	Dried	–	–	–	17	Very weak
F2	Dried and calcined	–	–	–	24	Very weak
C1	Dried	4	12	7	29	High
C1	Dried and calcined	6	20	8	27	High
C2	Dried	3	14	7	24	High
C2	Dried and calcined	3	24	11	56	High
FC1	Dried	4	13	7	17	Moderate
FC1	Dried and calcined	4	24	11	31	Moderate
FC2	Dried	–	–	–	15	Weak
FC2	Dried and calcined	–	–	–	14	Very weak

d_{min}, the minimum carbon nanotubes diameter; d_{max}, the maximum carbon nanotubes diameter; d_{CNTs}, the average carbon nanotubes size calculated from the observation of 30 carbon nanotubes.

could accelerate the sintering of the metal particles [20,21]. For instance, the presence of NO_3^- anions seems to favour sintering and the formation of larger particles.

A correlation is observed between the active metal particle size and the carbon nanotubes diameter, see Tables 2 and 3. Catalysts with large particles, i.e., FC1-dc and C2-dc with d_{TEM} of 8 and 12 nm, respectively, lead to a carbon deposit containing carbon nanotubes with large diameters corresponding to d_{TEM} of 11 nm for each catalyst. Catalysts with smaller particles, i.e., as F1-d and FC1-d with d_{TEM} of 4 and 5 nm, lead to a carbon deposit containing carbon nanotubes with smaller diameters of 7 nm each. Such a correlation, which has been already reported [22,23] in the literature, can be explained by the mechanism described by Dai et al. [22] and Li et al. [23] in which carbon nanotubes grow on active metal particles. This mechanism, which leads directly to a relationship between the nanotube diameter and the metal particle size, also explains the lower activity for carbon nanotube production with catalysts containing smaller metal particles. In the latter case some of the particles are simply too small to catalyze the growth of nanotubes. Observed carbon nanotubes have a minimal diameter of 0.4 nm [24], since then, this minimal carbon nanotubes diameter could explain the minimal size of particles required for carbon nanotubes production activity. This is the case for the F2-d, F2-dc, FC2-d, and FC2-dc catalysts that have small metal particle diameters which d_{TEM} are 3, 5, 3 and 4 nm, respectively. For these catalysts, only a few carbon nanotubes were found in the carbon deposit. Another possible explanation is that the small particles could be encapsulated by the support during the synthesis and would not be accessible to the reactants.

Fig. 7. TEM micrograph of the carbon deposit of C2-dc (352,000×).

Moreover, a comparison between the XRD results reported in Table 2 and the carbon nanotubes/amorphous carbon ratio reported in Table 3 seems to indicate that active metal particles must be crystalline in order to be active in carbon nanotubes production. Indeed, all catalysts characterized by an absence of XRD peaks corresponding to iron and/or cobalt containing phases exhibit a weak or moderate carbon nanotubes/amorphous carbon ratio. Such an absence is not necessarily because the particles are too small to be detected. It could also be due to the amorphous nature of the particles. Considering particle size only, sample FC1 should exhibit diffraction peaks as do samples F1 and C1 which do not contain larger particles according to the TEM results. A difference between the particles in FC1 and those in F1 and C1 could be the crystallinity, i.e., the particles in FC1 may be amorphous whereas the particles in F1 and C1 may be crystalline. Indeed, crystallinity may be a necessary condition for the catalytic formation of carbon nanotubes. This requirement could be explained by the organized structure of carbon nanotubes which may require the regular catalytic surface of a crystalline material to be formed.

The metal particle size can also be correlated with the catalytic activity of the catalysts, see Tables 2 and 3. Indeed, the highest carbon deposits of 43 and 56% are obtained with F1-dc and C2-dc, respectively, catalysts that have large active metal particles which d_{TEM} are 7 and 12 nm, respectively. In contrast, the smaller carbon deposits of 17, 24, 15, and 14% are obtained with F2-d, F2-dc, FC2-d, and FC2-dc, respectively, catalysts that have small active metal particles which d_{TEM} are 3, 5, 3 and 4 nm, respectively. Previous studies indicate that better dispersion of the supported metal could reduce the amount

of carbon deposited [25,26]. The catalysts presented here, which are obtained from sol–gel processing, have a very high surface area, see Table 2. It is worth noting that the two best catalysts, F1-dc and C2-dc, have both large S_{BET} surface areas of more than 270 m^2/g and large metal oxide particles of 7 and 12 nm, respectively. In the case of high dispersion, when the average metal oxide particle size is small, the carbon deposit is lower.

Moreover, the results presented in Table 3 indicate that the catalysts that yield a high carbon deposit, i.e., C2-dc, also produce a large quantity of carbon nanotubes. In contrast, catalysts that yield a low carbon deposit, i.e., FC2-dc, also produce only a small quantity of carbon nanotubes.

In this study, the catalytic activity of the metal species towards a carbon deposit is found to decrease in the order, Co > Fe > Fe–Co. The most active catalysts are the cobalt-supported ones. In these catalysts, Co_2AlO_4 is formed between the cobalt oxide and the Al_2O_3 catalyst support. This Co_2AlO_4 may be responsible for the better activity of the cobalt catalyst because the metal–support interactions have an extensive influence on the yield of the carbon deposit from chemical catalytic vapour deposition [27].

5. Conclusion

Fe, Co and Fe–Co/Al_2O_3 catalysts synthesized by a one step sol–gel method permit the production of carbon nanotubes by the ethylene chemical catalytic vapour deposition process. The catalytic activity of the metal species towards carbon deposit was found to decrease in the order Co > Fe > Fe–Co.

Different metal precursors – nitrate, acetylacetonate, and acetate complexes – were used to synthesize the various catalysts. The nature of the metal precursor influences their activity and selectivity. For instance, Fe/Al_2O_3 catalysts synthesized with $Fe(NO_3)_3$ as the precursor have a better activity and selectivity than Fe/Al_2O_3 catalysts synthesized from $Fe(acac)_3$. $Co(acac)_2$ leads to the formation of Co_2AlO_4 between the cobalt oxide and the Al_2O_3 support in the Co/Al_2O_3 catalysts, a formation that helps promote the production of carbon nanotubes. The nature of the metal precursor also influences the extent of iron or cobalt oxide particle growth during the sintering process and, as a consequence, its particle size.

The metal oxide particle size can be related to the catalytic activity and a minimal size for the metal oxide particles seems to be necessary to effectively produce carbon nanotubes. Indeed, an increase in the production of both amorphous carbon and carbon nanotubes results when the catalyst contains large metal oxide particles. In contrast, small metal oxide particles lead mainly to the production of amorphous carbon. Further, an extensive dispersion of the metal oxide on the catalyst support produces only amorphous carbon and is, as a consequence, unfavourable for the production of carbon nanotubes. Finally, the extent of the crystallinity of the metal oxide particles seems to be important in the production of carbon nanotubes.

Acknowledgements

KYT is grateful to the Belgian Fonds pour la Formation à la Recherche dans l'Industrie et dans l'Agriculture for a grant in support of her Ph.D. research. SL is indebted to the Belgian Fonds National de la Recherche Scientifique for a postdoctoral research position. The authors thank the Fonds National de la Recherche Scientifique, the Région Wallonne - Direction Générale des Technologies, de la Recherche et de l'Énergie -, the Ministère de la Communauté Française, and the Fonds de Bay for their financial support. The European Network of Excellence FAME is also acknowledged for its support for this work.

References

[1] M. Monthioux, V.L. Kuznetsov, Carbon 44 (2006) 1621.
[2] S. Ijima, Nature 354 (1991) 56.
[3] M.S. Dresselhaus, G. Dresselhaus, P.C. Eklund, Science of Fullerene and Carbon Nanotubes, Academic Press, San Diego, CA, 1995.
[4] E.T. Thostenson, Z. Ren, T.W. Chou, Comp. Sci. Technol. 61 (2001) 1899.
[5] N.V. Surovtsev, A.A. Kalinin, V.K. Malinovsky, Y.N. Pal'yanov, A.S. Yunoshev, Carbon 44 (2006) 2032–2038.
[6] H. Kathyayini, I. Willems, A. Fonseca, J.B. Nagy, N. Nagaraju, Catal. Commun. 7 (2006) 140–147.
[7] A. Dupuis, Prog. Mater. Sci. 50 (2005) 929.
[8] C. Laurent, E. Flahaut, A. Peigney, A. Rousset, New J. Chem. 22 (1998) 1229.
[9] H. Kathyayini, N. Nagaraju, A. Fonseca, J.B. Nagy, J. Mol. Catal. A 223 (2004) 129.
[10] M. Khoudiakov, M.C. Gupta, S. Deevi, Appl. Catal. A 291 (2005) 151.
[11] M. Pérez-Cabero, I. Rodriguez-Ramos, A. Guerrero-Ruiz, J. Catal. 215 (2003) 305.
[12] J. Geng, C. Singh, D.S. Shepard, M.S.P. Shaffer, B.F.G. Johnson, A.H. Windle, Chem. Commun. (2002) 2666.
[13] S. Lambert, C. Cellier, P. Grange, J.P. Pirard, B. Heinrichs, J. Catal. 221 (2004) 335.
[14] A.J. Lecloux, J.-P. Pirard, J. Non-Cryst. Solids 225 (1998) 143.
[15] D.H. Kim, S.I. Woo, J. Noh, O. Yang, Appl. Catal. A (2001) 69.
[16] C. Gommes, S. Blacher, C. Bossuot, P. Marchot, J.B. Nagy, J.P. Pirard, Carbon 42 (2004) 1473.
[17] C. Gommes, S. Blacher, N. Dupont-Pavlovsky, C. Bossuot, M. Lamy, A. Brasseur, D. Marguillier, A. Fonseca, E. McRae, J.B. Nagy, J.P. Pirard, Colloids Surf. A 241 (2004) 155.
[18] G. Bergeret, P. Gallezot, in: G. Ertl, H. Knözinger, J. Weitkamp (Eds.), Handbook of Heterogeneous Catalysis, Wiley–VCH, Weinheim, 1997, p. 432.
[19] A.J. Lecloux, in: J.R. Anderson, M. Boudart (Eds.), Catalysis: Science and Technology, vol. 2, Springer, Berlin, 1981, p. 171.
[20] B. Bachiller-Baeza, A. Guerrero-Ruíz, I. Rodríguez-Ramos, J. Catal. 229 (2005) 439.
[21] S. Balcon, S. Mary, C. Kappenstein, E. Gengembre, Appl. Catal. A 196 (2000) 79.
[22] H. Dai, A.G. Rinzler, D. Nikolaiev, A. Thess, D.T. Colbert, R.E. Smalley, Chem. Phys. Lett. 260 (1996) 471.
[23] Y. Li, W. Kim, Y. Zhang, M. Rolandi, D. Wang, H. Dai, J. Phys. Chem. B 105 (2001) 11424.
[24] N. Sano, M. Chhowalla, D. Roy, G.A.J. Amaratunga, Phys. Rev. B 66 (2002) 113403.
[25] L. Ji, S. Tang, P. Chen, H.C. Zeng, J. Lin, K.L. Tan, Pure Appl. Chem. 72 (2000) 327.
[26] X. Wu, P. Chen, J. Lin, K.L. Tan, Int. J. Hydrg. Energ. 25 (2000) 261.
[27] H. Kathyayini, N. Nagaraju, A. Fonseca, J.B. Nagy, J. Mol. Catal. A 223 (2004) 129.